Articles

Relationship between
normalized cross-correlation coefficient obtained
from shunt murmur and vascular resistance index

SHIN'E Yoshimasa[*], SASAKI Kazuma[1], NAKANE Noriaki[2],
OKU Tomoko[3], MOTOHASHI Yuka[3], YAMAUCHI Shinobu[4] and SATO Toshio[4]

I. Introduction

In hemodialysis patients, an arteriovenous fistula (AVF) is created to increase venous perfusion by enabling blood to flow directly into a vein from an artery via an arteriovenous anastomosis. Turbulence and vortices are generated downstream from the anastomosis, and continued pressure of this unnatural flow against vascular walls causes thickening of the vascular intima, resulting in frequent stenosis downstream from the anastomosis. Maintaining vascular access (VA) in good condition is vital for the continuation of hemodialysis treatment. A variety of VA management tools are therefore used to assess VA function in everyday clinical practice. We have previously reported measurements over time for shunt murmurs in hemodialysis patients, and have developed a new screening method for noninvasive assessment of the progression of stenotic lesions in terms of the normalized cross-correlation coefficient R, which expresses the frequency domain calculated from images obtained from the time-frequency analysis of shunt murmurs.

According to a questionnaire survey by the statistics and research committee of the Japan Association for Clinical Engineers technologists, approximately 50% of hemodialysis institutions had already installed diagnostic ultrasound equipment as of 2013. VA management now relies not only on physical signs obtained by visual examination, palpation, and auscultation, but also on measurements of the vascular resistance index (RI) and brachial artery flow volume (FV) on ultrasound. Ultrasound scanning enables the function and shape of the VA to be assessed simultaneously. As this system also shows a high detection rate for stenotic lesions, this is regarded as an advantageous method of testing in VA management. As stenosis progresses, systolic flow velocity increases and end-diastolic flow velocity decreases, and the flow velocity waveform measured in the brachial artery therefore exhibits a steeper slope. When stenosis is severe, flow velocity decreases rapidly after peaking in the systolic phase, causing

* SHIN'E Yoshimasa: Graduate student of Engineering, Department of Biomedical Engineering, Toin University of Yokohama. 1614, Kurogane-cho, Aoba-ku, Yokohama 225-8503, Japan
1 SASAKI Kazuma: Assistant Professor, Faculty of Medical Technology, Department of Clinical Engineering and Medical Technology, Niigata University of Health and Welfare , 1398 Shimami-cho, Kita-ku, Niigata-shi, Niigata 950-3198, Japan
2 NAKANE Noriaki: Visiting researcher, Faculty of Biomedical Engineering, Toin University of Yokohama
3 OKU Tomoko and MOTOHASHI Yuka: Lecturer, Faculty of Biomedical Engineering, Toin University of Yokohama
4 YAMAUCHI Shinobu: Associate Professor, Graduate School of Engineering, Faculty of Biomedical Engineering, Toin University of Yokohama
4 SATO Toshio: Professor, Faculty of Biomedical Engineering, Toin University of Yokohama

the appearance of a notch or retrograde component with negative velocity in the flow waveform. In addition, immediately before the VA becomes occluded, flow velocity falls to zero in the diastolic phase, and the severity of stenosis can therefore be estimated from this and other observations of the flow velocity waveform. However, measurement errors may arise in ultrasound scanning as a result of the observer's level of skill and various other factors, including ultrasound beam angle correction and sample volume designation required for blood flow measurement, and flattening of the vessel diameter due to compression by the probe. Diagnostic ultrasound units that visualize vessel diameter and are fitted with an assistive function that automatically adjusts the beam angle and sample width are thus now coming into clinical use. However, measurements of the FV and RI of the AVF of a single patient using several different devices fitted with such assistive functions reportedly yield different values as a result of device-specific variation. A requirement for pre-test calibration is now starting to be identified. Despite this requirement, an AVF model for use in calibration with the aim of resolving this problem has yet to be developed or commercialized, and there is thus an increasing need for the development of such an AVF model.

In this study, we created a prototype model simulating an AVF distal to the brachial artery and measured changes in RI and FV when the stenosis rate of the vein downstream from the anastomosis was increased in a graduated manner, with the objective of investigating the association between changes in the stenosis rate and R, RI, and FV.

II. Experimental Methods

As an AVF model to simulate a properly functioning VA, we cut off the ends of a Y-shaped tube connector with a 60° bifurcation angle at a dis-

tance of 10 mm from the bifurcation. To the cut-off end of the venous-side connector, we connected a TOUGHSiLON gel tube (Tanac Co., Ltd.) to simulate the cephalic vein. To the other arterial-side connector, we connected a silicone tube to simulate the radial artery. We then connected another Y-shaped tube connector to the tip of this silicone tube to create a further bifurcation, to one side of which we connected a TOUGHSiLON gel tube to simulate the brachial artery, and to the other side a silicone tube to simulate the ulnar artery. In the experiments, a clamp was attached to the tube simulating the ulnar artery. This clamp was opened or closed to reproduce the flow of blood in this artery. Next, to reproduce the process of reduced VA function due to progressive stenosis, we created stenosis parts made of round acrylic rods with holes through the middle, the diameter of which was progressively decreased from 4.8 mm to 1.2 mm in 20% increments. The AVF model was created by placing one of these stenosis parts within the venous-side connector of the Y-shaped tube connector. *Figure 1* shows the completed AVF model. Pulsatile flow of water containing microscopic air bubbles was circulated through this AVF model using a multifunctional pulsation pump (Alpha Flow EC-1, Fuyo Co., Ltd.). The multifunctional pulsation pump was set so that
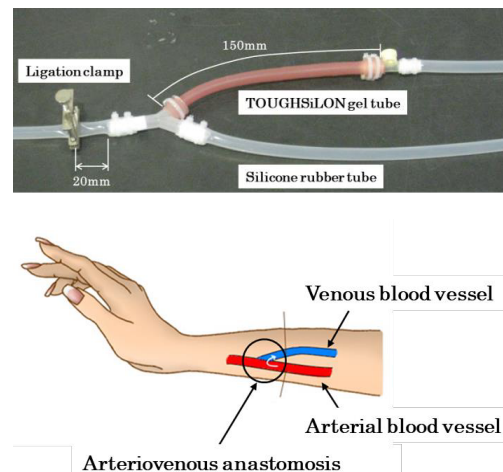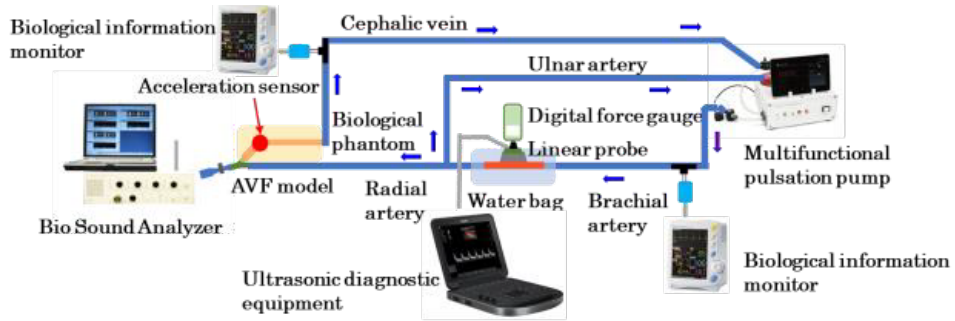

Fig.1 AVF model

Fig.2 Experimental system

the pulsatile flow through the model had a pulse rate of 60 beats/min, the duty ratio (expressing the proportions of systolic and diastolic phases of the heart) was 35%, systolic blood pressure was 70 mmHg, diastolic blood pressure was 10 mmHg, and venous pressure was 60 mmHg. A biological information monitor (BP-A308D, Omron health-care Co., Ltd.) was connected downstream of the outlet of the pulsation pump and downstream of the AVF model respectively to monitor pressure changes of pulsation flow. The TOUGHSiLON gel tube simulating the brachial artery was enclosed in a water bag, and the linear probe of an ultrasonic diagnostic equipment (Sonosite EdgeⅡ, Fujifilm Co., Ltd.) was applied from above to measure the blood flow velocity waveform.

The RI was calculated from the measured value using Equation (1), and FV was calculated using Equation (2).

$$RI = (PSV - EDV) / PSV \qquad (1)$$

$$FV \ (ml/min) = TAV \times A \times 60 \qquad (2)$$

In Equation (1), peak systolic velocity (PSV, cm/s) is the maximum blood flow velocity in the systolic phase, and end-diastolic velocity (EDV, cm/s) is the minimum blood flow velocity in the diastolic phase. In Equation (2), the time-averaged velocity (TAV, cm/s) is the mean velocity over time, and A denotes the cross-sectional area (cm^2) of the vessel. *Figure 2* shows the experimental system. The probe was fixed to an experimental
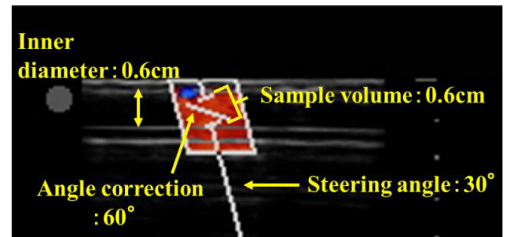

Fig.3 Measurement of blood flow velocity waveform with ultrasonic diagnostic equipment

stand to prevent dislodgement or a change in contact pressure during experiments. Contact pressure was adjusted to 10 N using a digital force gauge (DS2-200N, Imada Co., Ltd.). As shown in *Figure 3*, flow velocity waveforms were measured at a steering angle of 30°, sample volume of 0.6 cm, and angle correction of 60°. To measure simulated shunt murmurs generated in the veins of each AVF model, this part was embedded inside a biological phantom (food-quality konjac), and an accelerometer (TA-701T, Nihon Koden Co., Ltd.) was attached to the surface of the phantom. The simulated shunt murmurs were measured and recorded with the accelerometer and a Bio Sound Analyzer (BSA) that we have developed ourselves. Time-frequency analysis of the simulated shunt murmurs thus obtained was conducted by means of wavelet transformation using WaveletDisp and WaveletBitmapAnalyzer dedicated analysis software. The normalized cross-correlation coefficient R, which expresses changes in frequency domains between the images that resulted from this analysis, was then calculated. Flow rates of brachial
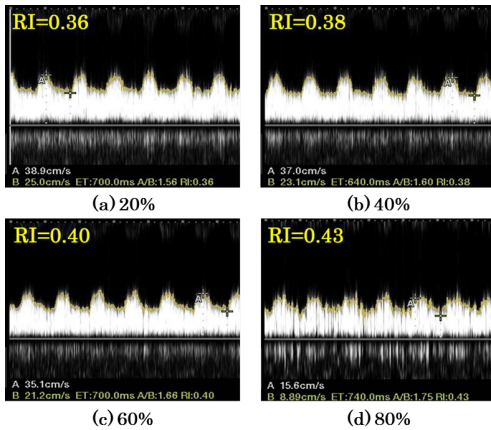
Fig. 4 Changes in flow velocity waveform for each diameter stenosis rate of AFV model (Ulnar artery downstream of the bifurcation with the brachial artery was occluded.)

artery, ulnar artery and VA were calculated by measuring the amount accumulated in one minute using a measuring cylinder respectively.

III. Experimental Results

The flow velocity waveform measured in the AVF model with an occluded ulnar artery downstream from the bifurcation with the brachial artery did not exhibit a rapid increase in flow velocity in the systolic phase or a gradual decrease in the diastolic phase (**Figure 4**). Qualitatively, this differed greatly from the flow velocity waveforms measured in hemodialysis patients. RI values hardly varied with different stenosis rates, with an
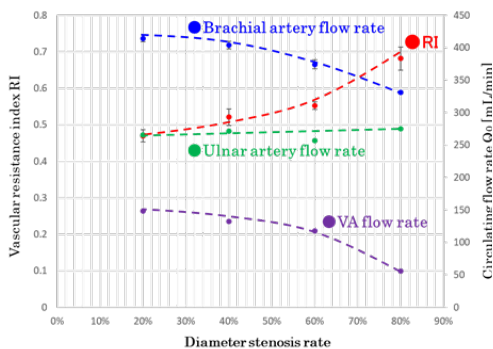

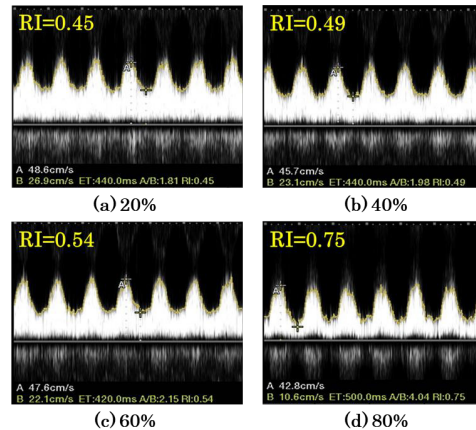**Fig. 6** Changes in RI and Q_0 due to changes in the diameter stenosis rate

Fig. 5 Changes in flow velocity waveform for each diameter stenosis rate of AFV model (Ulnar artery downstream of the bifurcation with the brachial artery was opened.)

RI of 0.36 at 20% stenosis, 0.38 at 40% stenosis, 0.40 at 60% stenosis, and 0.43 at 80% stenosis. The RI measured over time in hemodialysis patients increases with the progression of stenosis, but this pattern was not reproduced in the AVF model in which the ulnar artery downstream of the bifurcation with the brachial artery was occluded.

We then conducted the same measurements in an AVF model with a patent ulnar artery downstream from the brachial artery, and found that the flow velocity waveform exhibited an initial steep increase to a clearly detectable peak velocity in the systolic phase (**Figure 5**). Compared with stenosis rates of 20–60%, flow velocity at the severe stenosis rate of 80% increased to a higher value in the systolic phase, but with no detectable notch or
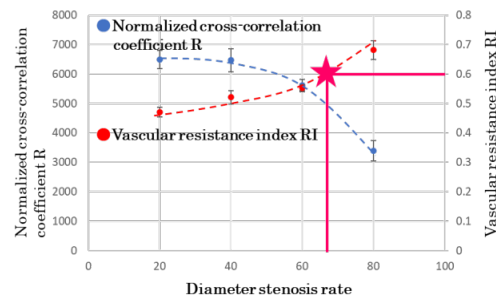

Fig. 7 Changes in R and RI due to changes in the diameter stenosis rate

retrograde component. RI tended to increase with increasing stenosis, with RI measured at 0.45 for 20% stenosis, 0.49 for 40% stenosis, 0.54 for 60% stenosis, and 0.75 for 80% stenosis. An examination of the results of RI and FV measurements at different stenosis rates also showed that although the brachial artery flow rate and VA flow rate decreased in linear fashion when the stenosis rate exceeded 50%, ulnar artery flow rate was almost unchanged (*Figure 6*). In terms of R values calculated from the simulated shunt murmurs measured downstream from the stenosis in AVF models, R was almost unchanged at approximately 6500 for stenosis rates of up to 40%, but when the stenosis rate exceeded 50%, R suddenly decreased to 5610 at 60% stenosis and 3391 at 80% stenosis (*Figure 7*). R and RI thus exhibited symmetrical changes with increasing rates of stenosis.

IV. Discussion

In this study, we created AVF models simulating an AVF formed by an anastomosis between the radial artery downstream of the brachial artery and the cephalic vein. We used diagnostic ultrasonography to measure flow velocity waveforms in the brachial artery, and then used these waveforms to calculate RI and FV at different stenosis rates. Because the AVF model with an occluded ulnar artery did not reproduce the anatomical bifurcation of the arteries or their peripheral hemodynamics, neither a rapid increase in peak flow velocity during the systolic phase nor a decrease in flow velocity during the diastolic phase was apparent, and the model did not reproduce the flow velocity waveforms measured in actual hemodialysis patients. When we then conducted the same experiment in an AVF model with a patent ulnar artery, an initial steep increase in flow velocity was seen irrespective of changes in the stenosis rate, and peak flow velocity was easily detectable.

In the brachial artery flow velocity waveforms in the AVFs of dialysis patients, when the stenosis rate is less than 50%, the steep initial increase in flow velocity in the systolic phase is followed by a gentle decrease in the diastolic phase. When the stenosis rate exceeds 50%, however, flow velocity increases rapidly in the systolic phase, then suddenly drops heading into the diastolic phase. In the systolic phase, a retrograde component consistent with the notch also appears, and in patients in whom the AVF is occluded, the flow velocity reportedly falls to zero in the diastolic phase. A comparison of the flow velocity waveforms reported in that study with those obtained in our present study showed that in the flow velocity waveforms obtained from models with low stenosis rates, flow velocity rapidly decreased from the systolic to the diastolic phase, and the gradual decrease in flow velocity in the diastolic phase seen in dialysis patients was not reproduced. Qualitative differences were also evident at higher stenosis rates, with no evident rapid decrease in flow velocity, notch, or retrograde component in the diastolic phase. When the ulnar artery was made patent, however, fluid resistance peripheral to the brachial artery decreased and peak flow velocity increased. The values of RI measured in models with graduated stenosis rates therefore increased in a linear fashion when the stenosis rate exceeded 50%. At 80% stenosis, the RI was 0.75, corresponding to AVF failure. In clinical practice, a flow volume in the brachial artery of 500 ml/min is more or less correlated with RI = 0.6, and this value is used as a guideline in VA function screening. The value of RI = 0.75 obtained at 80% stenosis was a result that corresponded with the region in which vascular access intervention treatment is indicated. The model created in this study has scope for improvement, but offers the first experimental reproduction of the process by which the RI of the AVF in dialysis patients increases with the progression of stenosis. We have previously reported that chang-

es in R values over time as calculated from shunt murmurs measured in dialysis patients are highly consistent with changes in R as measured from AVF models with graduated stenosis rates, and that 50% can be used as one guideline for a cut-off value for stenosis. In AVF models produced in this study, an RI value of 0.6–0.7 was equivalent to 70–80% stenosis when the length of the stenotic part was 10 mm. The R calculated from simulated shunt murmurs under these conditions was approximately 5000. R is easily calculated from shunt murmurs recorded with an electronic stethoscope or similar device, and can thus be used to provide a rough estimation of RI and stenosis diameter. This may contribute to improvements in the accuracy of screening for stenotic lesions.

V. Conclusion

In this study, we created an AVF model in which the brachial artery was bifurcated with a Y-shaped connector, with one side of the bifurcation simulating the ulnar artery and the other an anastomosis between the radial artery and cephalic vein. We inserted acrylic rods as simulated stenotic lesions downstream from the anastomosis in this model, with rates of stenosis graduated in 20% increments, and calculated the RI and FV from the flow velocity waveforms measured in AVF models with different stenosis rates. We found that RI increased as the stenosis rate increased, a result that experimentally reproduced the changes in RI seen in the AVFs of hemodialysis patients as a result of the progression of stenosis. The fact that R, our proposed coefficient that expresses the frequency domains of shunt murmurs, and RI both change markedly when the stenosis rate exceeds 50% suggests that monitoring changes in R over time may also enable the estimation of changes in RI and the stenosis rate.

[Notes]

1) Sasaki K, Yamauchi S, Motohashi Y, Sato T and Agishi T: Vascular access function assessment by combination of normalized cross-correlation coefficient and duration time. Toin University of Yokohama Research Bulletin 2018; 38: 97–104.

2) Domenico S, Filippo B, Placido M, Narayana P, David B, Francesco S, Carlo Alberto R, Valeria C and Michele B: Vascular access for hemodialysis: current perspectives, Int J Nephrol Renovasc Dis. 2014; 7: 281–294.

3) Massimo T, Lucia B, Marco C, Simine A, Ettore P, Vittoria E, Giuseppe S and Ciro E: Vascular access, complications and survival in incident hemodialysis patients, Kidney Dial. 2021; 1: 88–99.

4) Sasaki K, Shin'e Y, Oku T, Yamauchi S, Motohashi Y, Sato T and Agishi T: Performance evaluation of arteriovenous fistula models simulating shunt murmurs in hemodialysis patients, Toin University of Yokohama Research Bulletin 2020; 42: 155–161.

5) Amanda V, Kathryn M: Vascular access monitoring and surveillance: an update, Adv Chronic Kidney Dis. 2015; 22(6): 446–452.